Calcified Tissue International (2018) 103:324–337
https://doi.org/10.1007/s00223-018-0425-1

ORIGINAL RESEARCH

Glycyrrhizin Suppresses RANKL-Induced Osteoclastogenesis and Oxidative Stress Through Inhibiting NF-κB and MAPK and Activating AMPK/Nrf2

Zhikun Li[1] · Chao Chen[1] · Xiaodong Zhu[1] · Yifan Li[1] · Ronghua Yu[1] · Wei Xu[1]

Received: 6 February 2018 / Accepted: 2 April 2018 / Published online: 2 May 2018

Abstract

The treatment for osteoporosis involves inhibiting bone resorption and osteoclastogenesis. Glycyrrhizin (GLY) is a triterpenoid saponin glycoside known to be as the most medically efficacious component of the licorice plant. It has strong anti-inflammatory, antioxidant, and antitumor properties. We investigated the effect of GLY on osteoclastogenesis, bone resorption, and intracellular oxidative stress and its molecular mechanisms. In vitro osteoclastogenesis assays were performed using bone marrow monocytes with and without glycyrrhizin. We also evaluated the effects of glycyrrhizin on the secretion of TNF-α, IL-1β, and IL-6 in LPS-stimulated RAW 264.7 cells using ELISA. The effects of glycyrrhizin on the expression of osteoclast-related genes, such as *Nfatc1, c-fos, Trap*, and cathepsin K (*CK*), were investigated by RT-PCR. Intracellular reactive oxygen species (ROS) were detected in receptor activator of nuclear factor kappa-B ligand (RANKL)-stimulated osteoclasts in the presence and absence of glycyrrhizin. During the inhibition of osteoclastogenesis by glycyrrhizin, phosphorylation of AMPK, Nrf2, NF-κB, and MAPK was analyzed using western blotting. Our results showed that glycyrrhizin significantly inhibited RANKL-induced osteoclastogenesis, downregulated the expression of NFATc1, c-fos, TRAP, CK, DC-STAMP, and OSCAR, and inhibited p65, p38, and JNK. Glycyrrhizin was found to significantly decrease the secretion of inflammatory cytokines (TNF-α, IL-1β, and IL-6). Additionally, glycyrrhizin reduced the formation of ROS in osteoclasts by inducing AMPK phosphorylation and nuclear transfer of NRF2, resulting in an upregulation of antioxidant enzymes, such as HO-1, NQO-1, and GCLC. In summary, we found that glycyrrhizin inhibited RANKL-induced osteoclastogenesis. It was also indicated that glycyrrhizin could reduce oxidative stress by inhibiting the MAPK and NF-κB pathways and activating the AMPK/NRF2 signaling. Therefore, glycyrrhizin may be used as an effective therapeutic agent against osteoporosis and bone resorption.

Keywords Osteoclast · Glycyrrhizin · AMPK · Reactive oxygen species · Nrf2

Abbreviations

AMPK	AMP-activated protein kinase
ROS	Reactive oxygen species
NFATc1	Nuclear factor of activated T cells 1
JNK	c-Jun N-terminal kinase
NF-κB	Nuclear factor kappa B
Nrf2	Nuclear factor-erythroid 2-related factor 2
HO-1	Heme oxygenase-1
TNF-α	Necrosis factor-α
RANKL	Receptor activator of nuclear factor kappa-B (NF-κB) ligand
MAPK	Mitogen-activated protein kinase
M-CFS	Macrophage colony-stimulating factor
TRAP	Tartrate-resistant acid phosphatase
BMM	Bone marrow monocytes
GAPDH	Glyceraldehyde 3-phosphate dehydrogenase
CK	Cathepsin K
CTR	Calcitonin receptor

Zhikun Li and Chao Chen have equally contributed to this study.

Electronic supplementary material The online version of this article (https://doi.org/10.1007/s00223-018-0425-1) contains supplementary material, which is available to authorized users.

✉ Wei Xu
XW2107@shtrhospital.com

[1] Department of Spine Surgery, TongRen Hospital, School of Medicine, Shanghai Jiao Tong University, 1111 Xianxia Road, Shanghai 200336, People's Republic of China

DC-STAMP	Dendrocyte expressed seven transmembrane protein
OSCAR	Osteoclast-associated immunoglobulin-like receptor

Introduction

Bones are always in a state of dynamic metabolism due to simultaneous activated osteogenesis and bone resorption, which are executed by osteoblasts and osteoclasts, respectively [1]. Bone formation and resorption collectively govern the normal bone mass. Osteoclasts are special multinucleated macrophages that are formed by the fusion of monocytes derived from bone marrow hematopoietic stem cells and are mainly responsible for bone resorption [2]. An increase in the number or function of osteoclasts leads to osteoporosis, which significantly reduces bone mineral density and results in the formation of thin trabecular bone, eventually, increasing the risk of bone fractures.

Numerous studies have revealed that accumulative intracellular oxidative stress induced by reactive oxygen species (ROS) triggers cellular dysfunction, and may lead to inflammation, cancer, and aging, if the physiological antioxidant defense system fails to scavenge the ROS duly [3]. Specifically, it has been repeatedly reported that ROS played a critical role in osteoclastogenesis and bone resorption by RANKL-mediated activation of NADPH oxidase (NOX), TRAF6, and Rac1 by RANKL [4–6]. Nuclear factor-erythroid 2-related factor 2 (Nrf2) is the key transcription factor that regulates the generation of cytoprotective antioxidants including cytoprotective enzymes including heme oxygenase-1 (HO-1), NAD(P)H: quinone reductase (NQO-1), γ-glutamyl cysteine synthetase catalytic subunit (GCLC), and modifier subunit (GCLM), all of which are ROS scavengers [7, 8]. AMP-activated protein kinase (AMPK) has also been demonstrated to be a critical factor in oxidative response, inflammation, and tumorigenesis [9–11].

Studies have shown that many small molecular compounds derived from natural products have good pharmacological benefits that include antioxidant, antiaging, anti-inflammatory, and antitumor effects [12–15]. Certain compounds, including Carnosic acid, Avenanthramides, and Sodium hydrosulfide, are known to effectively inhibit osteoclast differentiation to prevent excessive bone resorption by inducing Nrf2/HO-1, and eliminate ROS and oxidative stress in osteoclasts [16, 17]. Recently, accumulative researches revealed that glycyrrhizin (GLY), a triterpenoid saponin glycoside known as the most efficacious component of the licorice plant, possesses multiple pharmacological properties including anti-inflammation, antitumor, antiaging, and antioxidative properties [18–21]. However, the scope of using GLY for the treatment of osteoporosis and other osteoclast-related diseases has not been extensively studied.

In the current study, we investigated the effect of GLY on the generation of ROS and the attenuation of RANKL-induced oxidative stress within osteoclasts. Our results demonstrated that glycyrrhizin inhibited osteoclastogenesis by suppressing NF-kB and MAPK in a dose-dependent manner. Furthermore, AMPK/Nrf2 were activated by the inhibitory effect of GLY, resulting in upregulation of antioxidants including HO-a, NQO1, and GCLC.

Materials and Methods

Reagents

Glycyrrhizin (purity, > 98%, as determined by high-performance liquid chromatography; Fig. 1a) was purchased from MeilunBio Co. (Dalian, Liaoning, China). It was stored at − 20 °C without direct exposure to light after it was dissolved in dimethyl sulfoxide supplied by Sigma-Aldrich (St. Louis, MO, USA). TRAP staining kit, Triton X-100, and 40,6-diamidine-20-phenylindole dihydrochloride (DAPI) were also provided by Sigma-Aldrich. Recombinant mouse RANKL and M-CSF were purchased from R&D Systems (Minneapolis, MN, USA). Alpha Modification of Eagle's Medium (α-MEM) was obtained from HyClone (Logan, UT, USA). Penicillin–streptomycin solution, trypsin-ethylenediaminetetraacetic acid solution (0.25%), and fetal bovine serum (FBS) were obtained from Gibco (Gaithersburg, MD, USA). Cell counting kit-8 (CCK-8) was provided by Dojindo Molecular Technology Inc. (Kumamoto, Japan). RNA extraction kit (RNeasy kit) was obtained from Qiagen (Valencia, CA, USA). Specific primary and secondary antibodies, including IkBα, P-IkBα, ERK, p-ERK, JNK, p-JNK, p38, p-p38, Akt, p-Akt, GSK3β, p-GSK3β, AMPK, p-AMPKα1, Nrf2, HO-1, NQO1, GCLC, GCLM, Lamin B, GAPDH, were purchased by Cell Signaling Technology (Danvers, MA, USA) and Santa Cruz Biotechnology (Santa Cruz, CA, USA). Hydroxyapatite-coated plates were purchased from Corning Life Science (St. Lowell, MA, USA). Compound C (Dorsomorphin) was used as AMPK inhibitor provided by Selleck Chemicals (Houston, TX, USA).

Isolation of Mouse Bone Marrow-Derived Monocytes (BMMs) and Cell Culture

All experiments were approved by the Ethics Committee of Tongren Hospital affiliated with Shanghai Jiao Tong University School of Medicine (Shanghai, China). All the protocols used were in accordance with the guidelines and procedures authorized by the Animal Care and Use Committee of

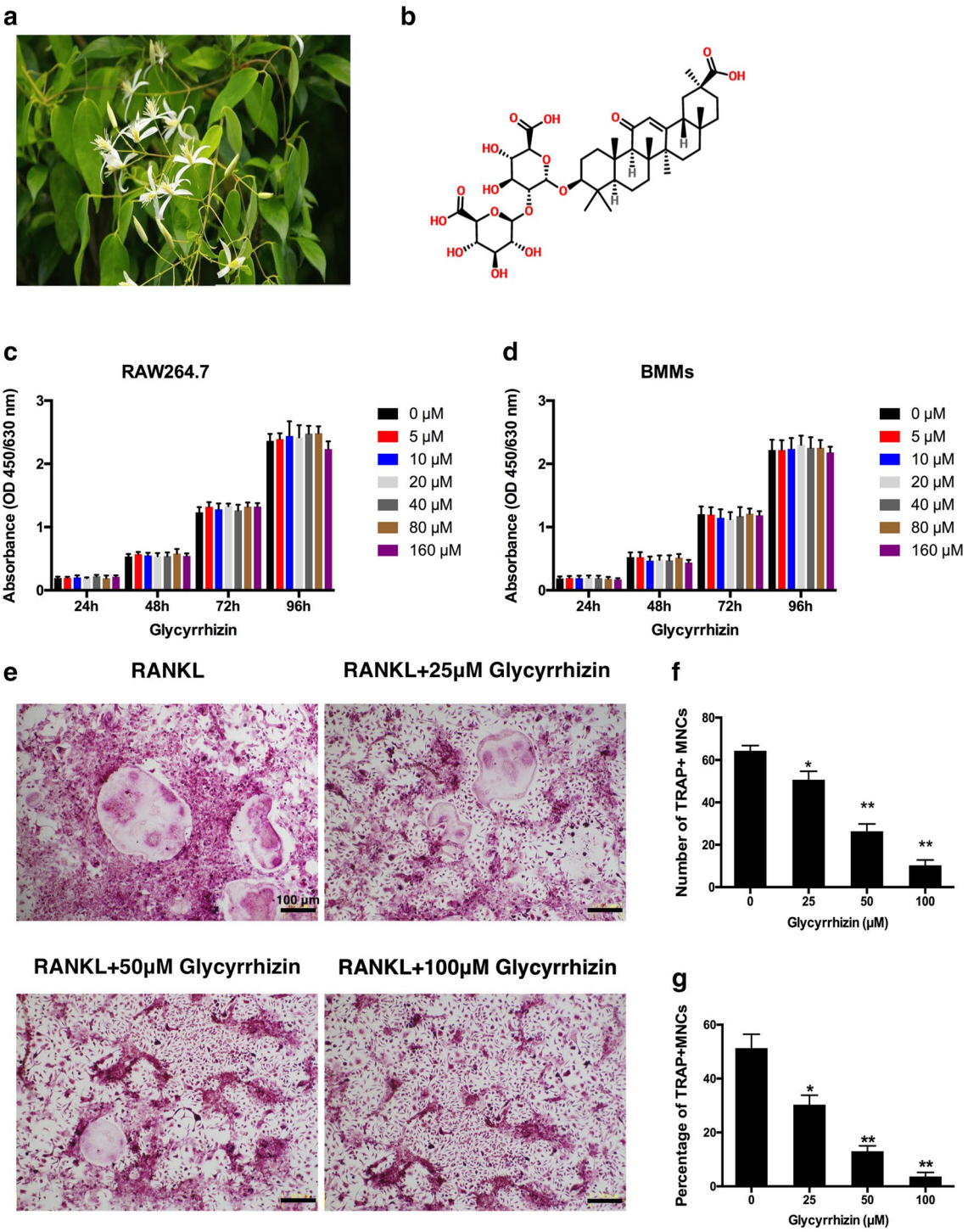

Fig. 1 Effect of glycyrrhizin on osteoclastogenesis in vitro. **a** Picture of *Glycyrrhiza uralensis* Fisch, **b** chemical structure of glycyrrhizin, **c, d** cell viabilities of RAW264.7 cells and BMMs after treatment with GLY for 24, 48, 72, or 96 h were detected using Cell Counting Kit-8 (CCK-8). **e** MNCs were incubated with RANKL and glycyrrhizin (0, 25, 50, or 100 μM) and osteoclasts were identified from the TRAP staining test. **f, g** Number and percentage of TRAP-positive MNCs. Asterisk indicates $p < 0.05$, double asterisk indicates $p < 0.01$

Shanghai Jiao Tong University School of Medicine. Primary BMMs were isolated from bone marrow aspirates of male C57BL/6 mice (6–8 weeks old) as described previously [22]. Briefly, bone marrow cells were isolated from aspirates of the tibiae and femurs of the mice. The cells were incubated in a culture dish (diameter, 10 cm) containing α-MEM, 10%

(v/v) FBS, and 30 ng/ml M-CSF at 37 °C in a humidified atmosphere (5% CO_2, 95% air) for 12–24 h. Next, the suspension of non-adherent cells was collected and reseeded in another 10-cm dish and cultured. After 3 days of incubation, the medium containing non-adherent cells (e.g., hemocytes and lymphocytes) and impurities was discarded and the adherent cells were used as BMMs. After another 3–4 days of culture until 90% confluence was reached, the BMMs were harvested by trypsin digestion and seeded into culture plates or dishes for further experiments.

Cell Viability Assay

Cell Counting kit-8 (CCK-8, Dojindo, Kumamoto, Japan) was used to evaluate cell viability. Briefly, RAW264.7 cells and BMMs were seeded in four 96-well plates with or without glycyrrhizin (0, 5, 10, 20, 40, 80, or 160 μM) for 24, 48, 72, or 96 h. Culture media were then replaced with those containing 30 ng/ml M-CSF, followed by incubation for 48 h. Next, the media were replaced with 10% CCK-8 solution (100 μl/well), after which the plates were incubated for 2 h at 37 °C. Absorbance was immediately measured at 450 nm (630 nm as reference) using a BioTek Synergy HT spectrophotometer. Each experiment was repeated three times. Results have been expressed as increases or decreases in cell number over different concentrations of glycyrrhizin.

In Vitro Osteoclastogenesis Assay

BMMs were seeded at 1×10^4/well in triplicates in 96-well plates for 24 h until they adhered to the plates. Culture media were replaced with fresh media containing 30 ng/ml M-CSF, 100 ng/ml RANKL, and varying non-cytotoxic concentrations of glycyrrhizin (0, 25, 50, or 100 μM). These media were changed every other day. After 7 days, the cells were fixed with 4% paraformaldehyde for 30 s, stained using TRAP kit according to the manufacturer's instructions, incubated for 1 h at 37 °C, and analyzed under a microscope. TRAP-positive multinucleated cells (MNCs) (nuclei, > 3) were counted as osteoclasts. The percentage of TRAP-stained MNCs per area (/mm^2) was measured using Image-Pro Plus 6.0 software. Each experiment was repeated three times [23].

F-actin Ring Formation Assay

BMMs were seeded at 8×10^4/dish in confocal culture dishes (diameter, 35 mm). 24 h later, by which time the cells had adhered to the dishes, the culture media were replaced with fresh media containing M-CSF and RANKL with or without glycyrrhizin (0, 50, or 100 μM). The cells were then cultured for 7 days. Next, the cells were fixed with 4% paraformaldehyde for 15 min, permeabilized with 0.1% (v/v) Triton X-100 for 5 min, and washed with phosphate-buffered saline (PBS) three times. F-actin was stained with rhodamine-conjugated phalloidin (1:100; Invitrogen Life Technologies, Carlsbad, CA, USA) diluted with 0.2% (w/v) bovine serum albumin-PBS at 37 °C for 1 h, followed by washing with PBS. Nuclei were stained with DAPI for 5 min at room temperature. A fluorescent microscope (Axiovert 200, Carl Zeiss, Oberkochen, Germany) was used to detect formed F-actin ring. Fluorescence images were processed using Zeiss ZEN software, and the number of intact F-actin rings was counted.

Hydroxyapatite Resorption Pit Assay

Hydroxyapatite resorption pit assay was performed using Corning Osteo Assay Surface 24-Well Plates (#3987; Corning Inc., Corning, NY, USA) coated at the bottom with hydroxyapatite. Next, 8×10^4 BMMs/well were seeded in the plates and media were changed with those containing 30 ng/ml M-CSF and 100 ng/ml RANKL with or without glycyrrhizin (0, 50, or 100 μM). Afterwards, the attached cells were cultured for 7 days at 37 °C in 5% CO_2 until the osteoclasts matured. The media were completely aspirated from the wells on day 7 and the cells were detached with trypsin. Von Kossa staining was performed in order to increase the contrast between pits and surface coating. Visual enumeration of pits was done using a microscope or software. The number of resorption pits (/mm^2) was counted, and the percentage of the resorption area was measured. Each experiment was repeated three times.

Enzyme-Linked Immunosorbent Assay (ELISA)

ELISA was performed to evaluate the effect of GLY on the secretion of inflammatory cytokines by LPS-stimulated RAW 264.7 cells incubated with or without glycyrrhizin (0, 50, or 100 μM). RAW 264.7 cells that were not treated with LPS served as the control group. ELISA kits were used for the experiments according to the manufacturer's instructions. Each experiment was repeated three times.

Reactive Oxygen Species (ROS) Assay

The level of intracellular reactive oxygen species (ROS) in BMMs was assessed using the cell-permeable dye dichlorofluorescein diacetate (DCFH-DA) and OxiSelect™ Intracellular ROS assay kit (Cell Biolabs, Inc., San Diego, CA, USA). BMMs were seeded at 5×10^5/well in six-well plates containing 30 ng/ml M-CSF and 100 ng/ml RANKL, with or without glycyrrhizin (0, 25, 50, or 100 μM). The plates were incubated for 24 h, followed by the addition of 10 μmol/l DCFH-DA to each well. Non-fluorescent DCFH

was converted to fluorescent DCFH-DA according to the amount of intracellular ROS generated. Fluorescence intensity was immediately measured using a BioTek Synergy HT spectrophotometer at excitation and emission wavelengths of 485 and 530 nm, respectively. Each experiment was repeated three times.

NF-kB and Are-Luciferase Assay

RAW 264.7 cells were stably transfected with NF-κB and ARE luciferase reporter constructed as described previously [24, 25]. Briefly, RAW 264.7 cells were seeded in 48-well plates and pretreated with glycyrrhizin (0, 25, 50, or 100 μM) for 1 h, followed by the addition of 100 ng/ml RANKL and incubation for 8 h. After cells were lysed with luciferase lysis buffer, luciferase activity was detected using Luciferase Assay Kit (Promega, Madison, WI, USA). Results have been presented as fold changes, which were obtained after normalization of data to that for the control group (0 mM glycyrrhizin group).

Nrf2 siRNA Transfection

For Nrf2 silencing, 5×10^5 cells per well of RAW 264.7 cells were grown in six-well plates. Effective siRNAs specific for mouse Nrf2 and negative control siRNA were purchased from Santa Cruz Biotechnology, Inc. (Santa Cruz, CA). When the confluence of cells reached approximately 50%, cells were then subjected to transient transfection with Nrf2-negative control siRNA and Nrf2-siRNA using the X-tremeGENE siRNA transfection reagent (Roche Applied Science), following the manufacturer's protocol. After 24 h, the transfected cells were treated with glycyrrhizin for 6 h, followed by lysis buffer for western blot analysis.

Total RNA Extraction and Real-Time Polymerase Chain Reaction (RT-PCR)

Quantitative PCR was used to measure the expression of specific genes during osteoclast formation. Briefly, BMMs were seeded at 5×10^5/well in six-well plates for total RNA extraction. The cells were incubated with 30 ng/ml M-CSF and 100 ng/ml RANKL, with or without 20 μM glycyrrhizin for 0, 1, 3, or 5 days. Total RNA was extracted using Qiagen RNeasy Mini kit according to the manufacturer's instructions. cDNA was synthesized from 1 μg of total RNA using reverse transcriptase (TaKaRa Biotechnology, Otsu, Japan). Real-time PCR was performed using SYBR Premix Ex Taq kit (TaKaRa) and an ABI 7500 Sequencing Detection System (Applied Biosystems, Foster City, CA, USA). Each reaction was run in triplicate. The mouse primer sequences for CK, calcitonin receptor (CTR), TRAP, DC-STAMP, OSCAR, c-fos, NFATc1, HO-1, NQO-1, and GAPDH are listed in Supplementary Table 1.

Western Blotting Analysis

The cells were lysed with radioimmunoprecipitation assay buffer (Beyotime, Shanghai, China) and 1% phenylmethylsulfonyl fluoride. Nuclear and cytoplasmic protein were isolated and extracted as previously reported [26]. Phosphatase Inhibitor Cocktail (#78441; Thermo Fisher, Waltham, MA, USA) was used to extract total protein after washing was done with PBS. The lysates were centrifuged at 12,000×*g* for 10 min and supernatants were collected. Protein concentrations in the samples were measured using BCA Protein Assay Reagent (Thermo Pierce, Rockford, IL, USA). Protein extracts were separated on sodium dodecyl sulfate–polyacrylamide gels and transferred onto polyvinylidene difluoride membranes (Millipore, Bedford, MA, USA). The membranes were incubated with primary antibodies at 4 °C overnight, after which secondary antibodies were added and incubated for 1 h at room temperature. Protein bands were detected using an Odyssey V3.0 image scanner (Li-COR. Inc., Lincoln, NE, USA). The intensity of each band was analyzed using ImageJ software.

NF-κB Activation Assay

4 × 103 cells/dish of RAW264.7 were seeded onto confocal dishes. After cells adhered, all culture media were replaced with or without pretreatment of GLY for 4 h. Then, three groups were stimulated with PBS or 100 ng/ml RANKL for 20 min. Untreated group was stimulated with PBS as control. Media were discarded and cells were fixed using 4% paraformaldehyde. Immunofluorescent stain was performed using the NF-kB/ p65 Activation Nuclear Translocation Assay Kit (Beyotime, Shanghai, China) according to manufacturer's instructions. The images were captured under an LSM5 confocal microscope (Carl Zeiss, Oberkochen, Germany).

Statistical Analysis

All results are expressed as mean ± standard deviation (SD) from at least three independent experiments. Statistical significance of data was analyzed using Student's *t* test or analysis of variance followed by Dunnett's test for post hoc analysis. SPSS 17.0 software (SPSS Inc., Chicago, IL, USA) was used for the statistical analysis. p values < 0.05 were considered statistically significant.

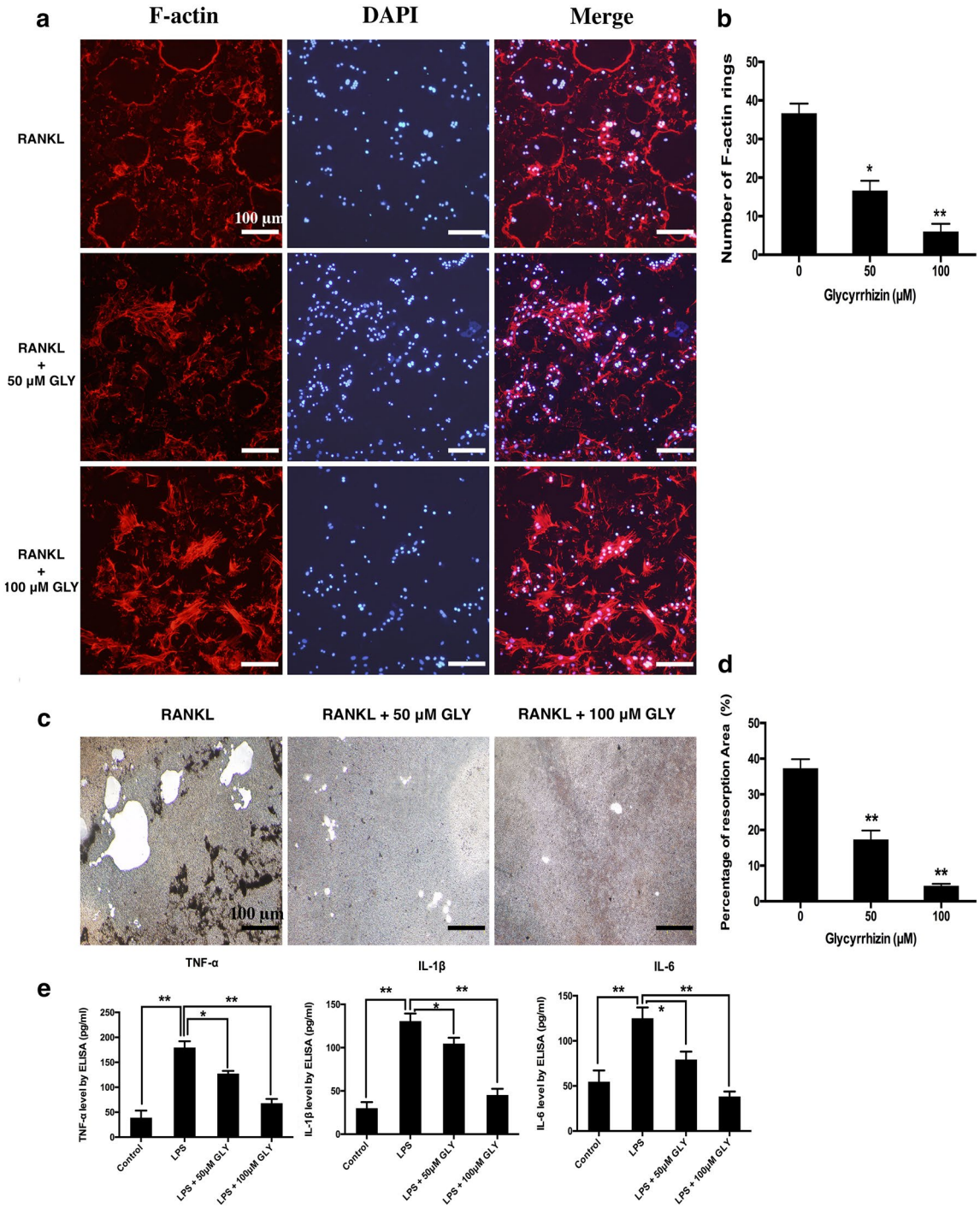

Fig. 2 Effects of glycyrrhizin on F-actin ring formation and bone resorption. **a, b** F-actin rings and cell nuclei in osteoclasts differentiated from BMMs were stained with 555 fluorescent phalloidin and DAPI, respectively, and counted. **c, d** BMMs were seeded in Corning osteo assay surface 24-well plates coated at the bottom with hydroxyapatite, and incubated with M-CSF, RANKL, and GLY for 9 days. **e** Secretion of inflammatory cytokines including TNF-a, IL-1β, and IL-6 was detected by ELISA. Asterisk indicates $p < 0.05$, whereas double asterisk indicates $p < 0.01$

Results

Glycyrrhizin Inhibits RANKL-Induced Osteoclastogenesis

The naturally active form of GLY in nature and chemical structure are shown in Fig. 1a, b, respectively. According to the results of the cell viability assay, proliferations of RAW264.7 cells and BMMs were not significantly reduced by glycyrrhizin even at concentration of 160 μM compared with those of control groups (0 μM), in which the OD values were 2.23 ± 0.12 (160 μM) versus 2.36 ± 0.11 (0 μM) and 2.18 ± 0.09 (160 μM) versus 2.21 ± 0.16 (0 μM) for RAW264.7 cells and BMMs, respectively, at 96 h ($p > 0.05$, Fig. 1c, d). Therefore, GLY was used at 0, 25, 50, or 100 μM concentrations in further experiments.

It has been demonstrated by TRAP staining that glycyrrhizin inhibited cell fusion and the formation of MNCs

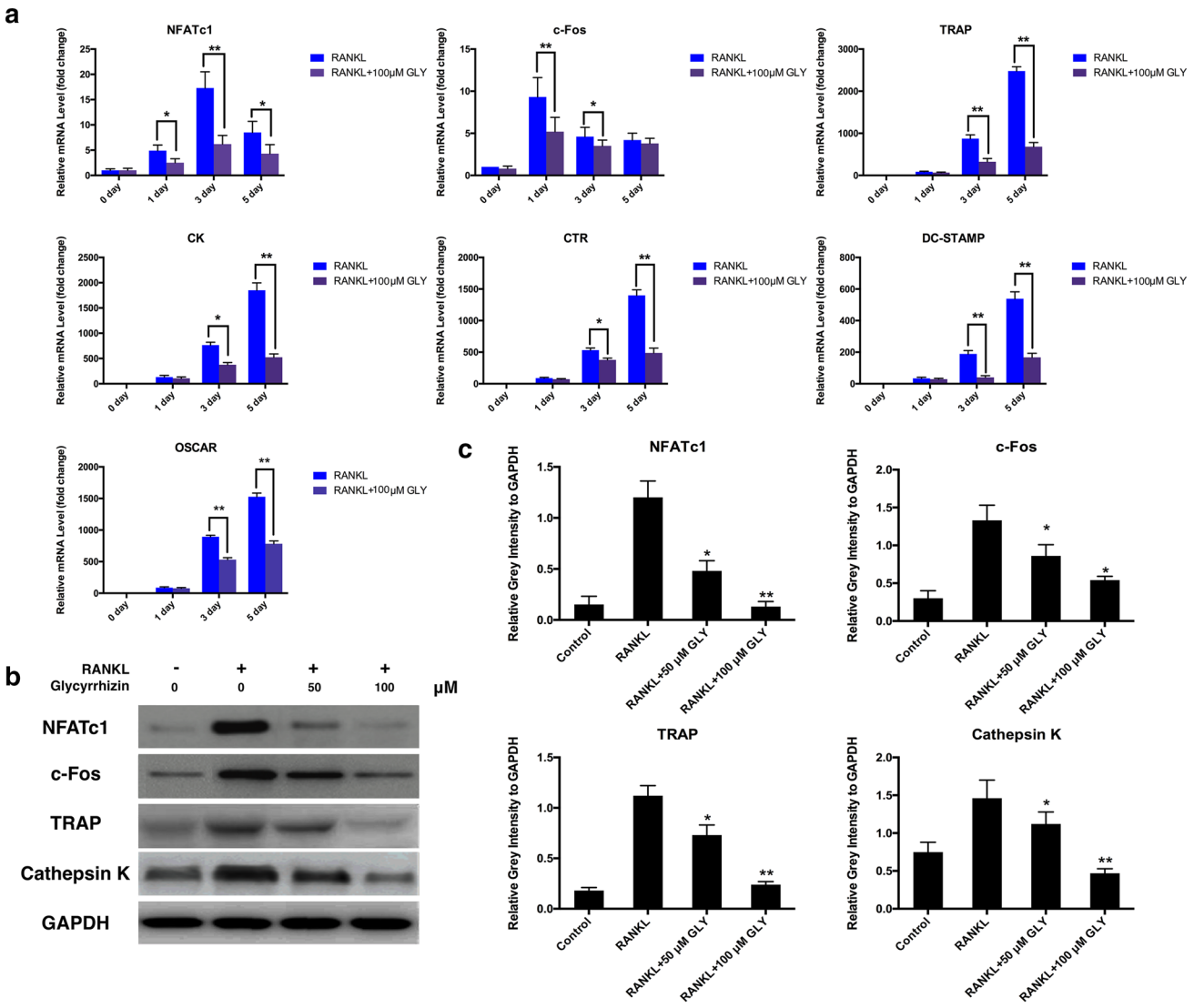

Fig. 3 Effect of glycyrrhizin on expression of osteoclastogenesis-related genes. **a** Differentiation and activity of osteoclast-related genes such as NFATc1, c-fos, TRAP, CK, CTR, DC-STAMP, and OSCAR were measured by real-time PCR. Asterisk and double asterisk indicate $p < 0.05$ and $p < 0.01$, respectively. **b, c** The protein of NFATc1, c-fos, TRAP, and CK were detected by western blotting

Fig. 4 Mechanisms of inhibitory effect of glycyrrhizin on osteoclastogenesis. **a** Phosphorylation of MAPK and NF-κB were evaluated by western blotting to further investigate the mechanism underlying the inhibition of osteoclastogenesis by glycyrrhizin. **b** Quantitative measuring the gray intensity of proteins compared to GAPDH. **c** Expressions of phosphorylated AMPK, Nrf2, and antioxidative enzymes were detected by western blotting. **d** Quantitative measuring the gray intensity of proteins compared to GAPDH or Lamin B. Asterisk indicates $p < 0.05$, double asterisk indicates $p < 0.01$. **e** Localization and transfer of NF-kB (p65) were detected in PBS, RANKL, and RANKL + GLY treated groups by immunofluorescence assay

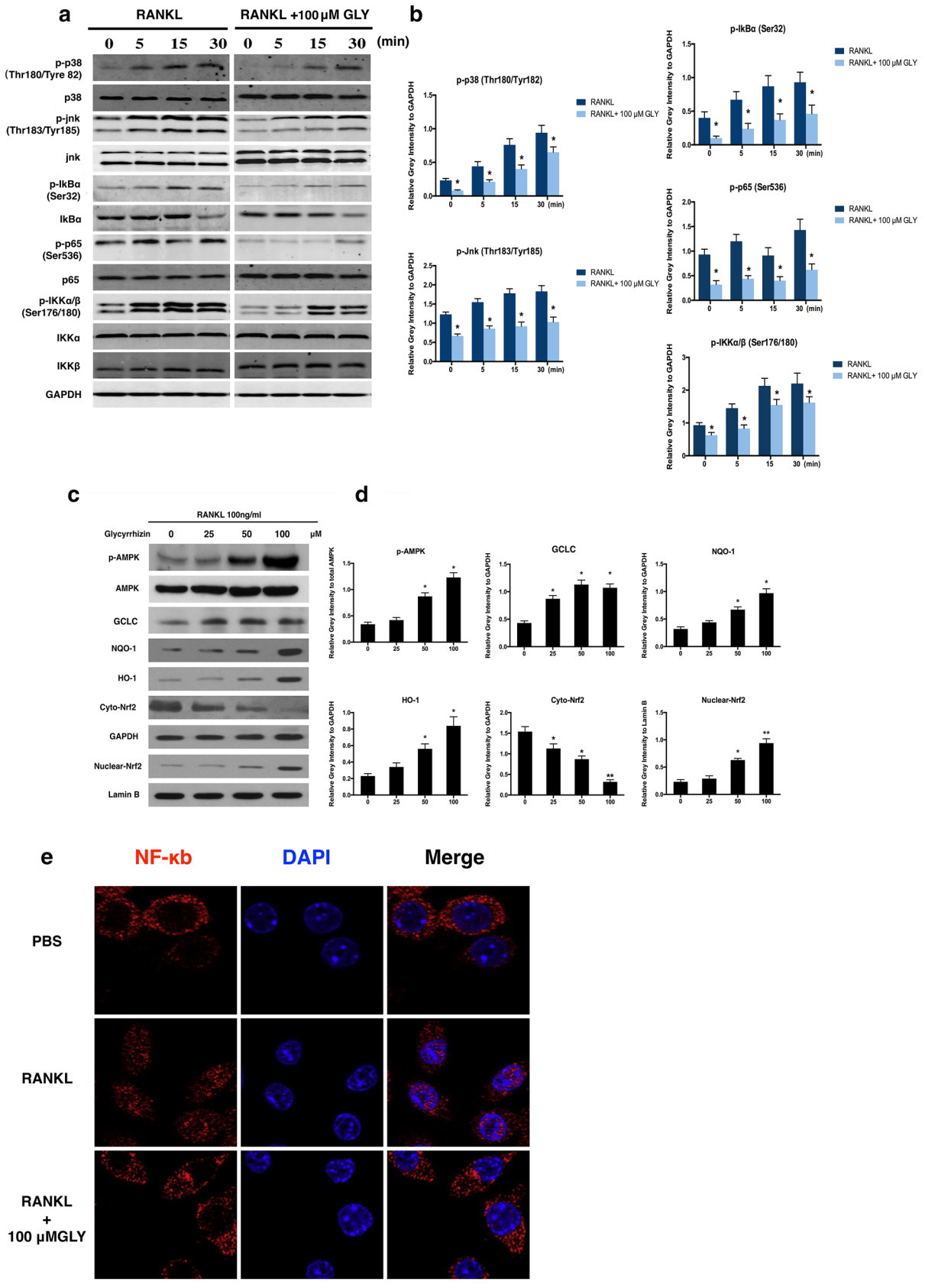
a
RANKL
RANKL +100 μM GLY
0 5 15 30 0 5 15 30 (min)
p-p38 (Thr180/Tyre 82)
p38
p-jnk (Thr183/Tyr185)
jnk
p-IkBα (Ser32)
IkBα
p-p65 (Ser536)
p65
p-IKKα/β (Ser176/180)
IKKα
IKKβ
GAPDH
b
p-p38 (Thr180/Tyr182)
p-Jnk (Thr183/Tyr185)
p-IkBα (Ser32)
p-p65 (Ser536)
p-IKKα/β (Ser176/180)
Relative Grey Intensity to GAPDH
RANKL
RANKL+ 100 μM GLY
30 (min)
c
RANKL 100ng/ml
Glycyrrhizin 0 25 50 100 μM
p-AMPK
AMPK
GCLC
NQO-1
HO-1
Cyto-Nrf2
GAPDH
Nuclear-Nrf2
Lamin B
d
p-AMPK
GCLC
NQO-1
HO-1
Cyto-Nrf2
Nuclear-Nrf2
Relative Grey Intensity to total AMPK
Relative Grey Intensity to GAPDH
Relative Grey Intensity to Lamin B
e
NF-κb
DAPI
Merge
PBS
RANKL
RANKL + 100 μMGLY

into osteoclasts in a dose-dependent manner (Fig. 1e). The number and percentage of TRAP-positive MNCs were accounted and analyzed. It was observed that the number and percentage of TRAP-positive MNCs in RANKL and 100 μM glycyrrhizin-treated group were 10.33 ± 2.31 and 3.67 ± 0.45%, respectively, while those were 64.33 ± 8.89 and 51.33 ± 7.16% in control group, respectively, which were significantly higher than those of GLY-treating group (Fig. 1f, g).

F-actin rings are microtubule and microfilament structures in cells, which play critical roles in seal zone formation and absorption of bone mineral matrix in osteoclasts. Results showed that the numbers of F-actin rings, visualized by phalloidin under a fluorescent microscope, was remarkably reduced in the glycyrrhizin-treated cells in a concentration-dependent manner (Fig. 2a, b). Specifically, numbers of F-actin formed during osteoclastogenesis were 36.67 ± 4.72, 17.21 ± 3.57, and 6.00 ± 1.39 in cells incubated with 0, 50, or 100 μM GLY, respectively. As a result of previous consequence, as expected, significantly fewer hydroxyapatite resorption pits were formed when osteoclasts were incubated with glycyrrhizin in comparison to that of control (Fig. 2c, d).

Moreover, the effect of GLY on secretion of inflammatory cytokines from RAW264.7 cells, not only precursors of osteoclasts but macrophages as well, was detected. Results of the ELISA experiment showed that concentrations of TNF-α in control, LPS, LPS + 50 μM GLY, and LPS + 100 μM GLY groups were 48.21 ± 8.12, 181.67 ± 23.33, 127.82 ± 11.75, and 59.12 ± 5.23 pg/ml, respectively. Meanwhile, the amount of IL-1β secreted by RAW264.7 cells from control, LPS, LPS + 50 μM GLY, and LPS + 100 μM GLY groups were 31.22 ± 5.83, 133.77 ± 21.86, 102.03 ± 16.72, and 42.52 ± 4.27 pg/ml respectively. Meanwhile, the concentrations of IL-6 in these groups were 55.37 ± 11.24, 127.81 ± 27.33, 78.24 ± 16.83, and 32.44 ± 6.11 pg/ml, respectively. Therefore, glycyrrhizin significantly inhibited the secretion of inflammatory cytokines including TNF-α, IL-1β, and IL-6 by LPS-stimulated RAW 264.7 cells (Fig. 2e).

Osteoclastogenesis-Related Genes Are Downregulated by Glycyrrhizin Through Suppression of NF-kB and MAPK

Results of RT-PCR revealed that after treatment of the cells with RANKL, GLY caused a significant and dose-dependent downregulation in the transcription of osteoclastogenesis-related genes such as NFATc1, c-fos, TRAP, CK, CTR, OSCAR, and DC-STAMP on day 1, 3, or 5 (Fig. 3a). In line with this, the expressions of proteins, including NFATc1, c-fos, TRAP, and CK, were noticeably inhibited by glycyrrhizin in a dose-dependent manner after stimulation of the cells with RANKL for 3 days (Fig. 3b, c).

NF-κB and MAPK both play critical roles in multiple physiological and pathological cellular behaviors including inflammation, carcinogenesis, proliferation, apoptosis, as well as osteoclastogenesis [27–29]. Therefore, we investigated effect of glycyrrhizin on them. The results indicated that glycyrrhizin tremendously suppressed phosphorylation of p38 MAPK, JNK, IKKα/β, and p65 NF-kB of pre-osteoclasts under stimulating by RANKL (Fig. 4a, b). Immunostaining of p65 in the activated NF-κB complex indicated the localization of p65 in the cytoplasm prior to stimulation of the cells by RANKL. Once the cells were stimulated by RANKL, the subcellular localization of p65 changed from cytoplasm to nucleus, thereby suggesting that RANKL activated the NF-κB complex. However, in the presence of GLY, the transfer of p65 from the cytoplasm to the nucleus was inhibited (Fig. 4e).

Inhibition of Osteoclastogenesis and Oxidative Stress by GLY Through the AMPK/Nrf2 Signaling Axis

Phosphorylation of AMPK (p-AMPK) and the expression of both cytoplasmic and nuclear Nrf2 were investigated by immunoblot. It was observed that GLY dose-dependently induced the phosphorylation of AMPK. Moreover, it was demonstrated that the cytoplasmic Nrf2, a critical regulator of intracellular antioxidants, was downregulated, while nuclear NRF2 was upregulated as compared to the untreated control. This suggests that GLY promotes the transfer of NRF2 from the cytoplasm to the nucleus for the regulation of downstream genes by inducing phosphorylation of AMPK. Accordingly, intracellular antioxidants such as HO-1, NQO-1, and GCLC increased in response to the treatment of glycyrrhizin in a concentration-dependent manner (Fig. 4c, d). The ROS in RANKL-induced osteoclasts were detected using DCFH-DA, a cell-permeable dye, and it was found that GLY significantly reduced the generation of ROS in a dose-dependent way (Fig. 5a). Luciferase assay revealed that glycyrrhizin simultaneously inhibited the transcription of NF-kB but promoting the transcription of Nrf2-ARE (Fig. 5b, c).

To further investigate the role of AMPK in the glycyrrhizin-mediated distribution of NRF2, a specific AMPK inhibitor called compound C (Dorsomorphin, CC) was used in another western blotting assay. Proteins were detected in four groups of cells treated with RANKL only (RANKL); treated with RANKL and glycyrrhizin (RANKL + GLY); treated with RANKL and compound C (RANKL + CC); treated with RANKL, glycyrrhizin, and compound C (RANKL + GLY + CC). The results suggested that the expression of p-AMPK in the RANKL + GLY + CC group

was significantly reduced in comparison with that in the RANKL + GLY group, indicating an effective attenuation of the activation of AMPK by glycyrrhizin in the presence of CC (Fig. 5d, e). While cytoplasmic NRF2 was remarkably upregulated in the RANKL + GLY + CC-treated cells, nuclear NRF2 was decreased in comparison to the RANKL + GLY-treated cells; this indicates that CC partly offsets the activation of p-AMPK and the transfer of NRF2 by GLY. In addition, the reduction in the ROS by GLY was found to be significantly restored after the inhibition of p-AMPK by CC (Fig. 5e).

Furthermore, the effect of CC on the GLY-induced suppression of osteoclastogenesis was monitored by TRAP staining. It was observed that the number of MNCs in RANKL + GLY group was dramatically less compared to that in the untreated control. The number of MNCs in RANKL + GLY + CC group was also less than the control but was significantly more than that in RANKL + GLY group. It can, therefore, be concluded that after getting remarkably suppressed by GLY, the formation of mature osteoclasts was partly restored by the addition of CC (Fig. 5f, h). Expression analyses of NFATc1 and c-fos proteins showed both the proteins were upregulated when treated with the RANKL + GLY + CC combination compared with that in the RANKL + GLY treatment, indicating the inhibition of osteoclastogenesis by GLY by inducing p-AMPK (Fig. 5d, g).

Silencing of Nrf2 Abolished the Protective Effect of Glycyrrhizin on RANKL-Induced Oxidative Stress

While oxidation is a fundamental risk factor in many disorders including osteoporosis [30, 31], Nrf2 is deemed as a master mediator of antioxidant enzymes including HO-1, NQO-1, GCLC, and GCLM. Therefore, we used siRNA targeting Nrf2 to study whether the inhibiting effect of glycyrrhizin on oxidative stress was Nrf2-dependent. In comparison to the control group, the remarkable property of GLY to eliminate intracellular ROS was effectively abolished in $Nrf2^{-/-}$ cells (Fig. 6b). Results of RT-PCR revealed that the GLY-induced upregulation of antioxidant enzymes, HO-1 and NQO-1, was also attenuated in $Nrf2^{-/-}$ group compared with control (Fig. 6c, d).

Discussion

The maintenance of normal bone mass largely depends on the homeostasis between the osteogenic effect of osteoblasts and the bone resorption activity of osteoclasts. Osteoclasts are multinucleated macrophages that are aggregated and fusion products of multiple monocytes that are stimulated by cytokines such as RANKL and TNF-α [32]. Recent studies on the molecular mechanisms of osteoclast differentiation and bone resorption-related genes, and in-depth molecular mechanisms have revealed many new targets for effective treatment of osteoporosis. The drugs currently used in osteoporosis reduce bone resorption primarily by inhibiting osteoclast formation. Currently available antioxidants that are used include bisphosphonates, selective estrogen receptor modulators, calcitonin, and estrogen [33, 34]. However, many recent studies have reported that some of these drugs cause serious health disorders such as breast cancer, endometritis, thromboembolism, hypercalcemia, osteonecrosis of the jaw, and atrial fibrillation [35, 36]. Some plant-derived small-molecule compounds have also been used to inhibit osteoclast differentiation and bone resorption, because of their anti-inflammatory, antioxidant, anti-inflammatory, and antitumor effects [12, 14, 15, 37].

In the present study, glycyrrhizin effectively inhibited RANKL-induced osteoclastogenesis in vitro. It was demonstrated by TRAP staining that glycyrrhizin significantly suppressed the formation of multinucleated giant cells. In addition, it reduced bone resorption in a dose-dependent manner, which was evidenced by the attenuation of F-actin ring formation in the osteoclasts and the bone resorption assay. The effects of glycyrrhizin on the expression of osteoclast-related genes were evaluated by RT-PCR and western blotting. These genes, including *NFATc1, c-fos, TRAP, CK, CTR, DC-STAMP, and OSCAR*, were significantly reduced by glycyrrhizin in a dose-dependent manner, especially on days 3 and 5 after the treatment with RANKL. Western blotting assays also indicated suppression in the levels of NFATc1, c-fos, TRAP, and CK.

As is well known, after RANKL binds to RANK, TRAF6 gets activated and is recruited to upregulate the expression of c-fos and NFATc1 via the NF-κB and the p38/JNK/ERK pathways. NFATc1 is the master molecule in osteoclastogenesis [29, 38, 39]. In the classical NF-κB pathway, RANKL activates phosphorylated IκB kinase (IKK) by activating an intracellular kinase, which then phosphorylates IκB to separate it from the p65-p50 dimer. This allows the dimer to translocate to the nucleus for upregulating the expression of downstream genes such as TRAP, NFATc1, and CK. Our results showed that glycyrrhizin decreased the phosphorylation of NF-κB (p65), IKK, p38, and JNK. We hypothesize that glycyrrhizin mediates the expression of downstream genes that regulate osteoclast differentiation through the NF-κB and MAPK signaling pathways.

Moreover, it has been reported that TRAF6 also plays a critical role in generation of reactive oxygen species (ROS) in osteoclasts induced by RANKL [6]. Redundant ROS in cells can trigger many disorders including inflammation, aging, metabolic disturbance, and osteoporosis [30, 31]. Therefore, the NRF2-mediated regulation of antioxidant enzymes, such as HO-1, NQO-1, GCLC, and GCLM, should be taken into consideration for preventing osteoporosis by reducing ROS levels. Additionally, AMPK has been

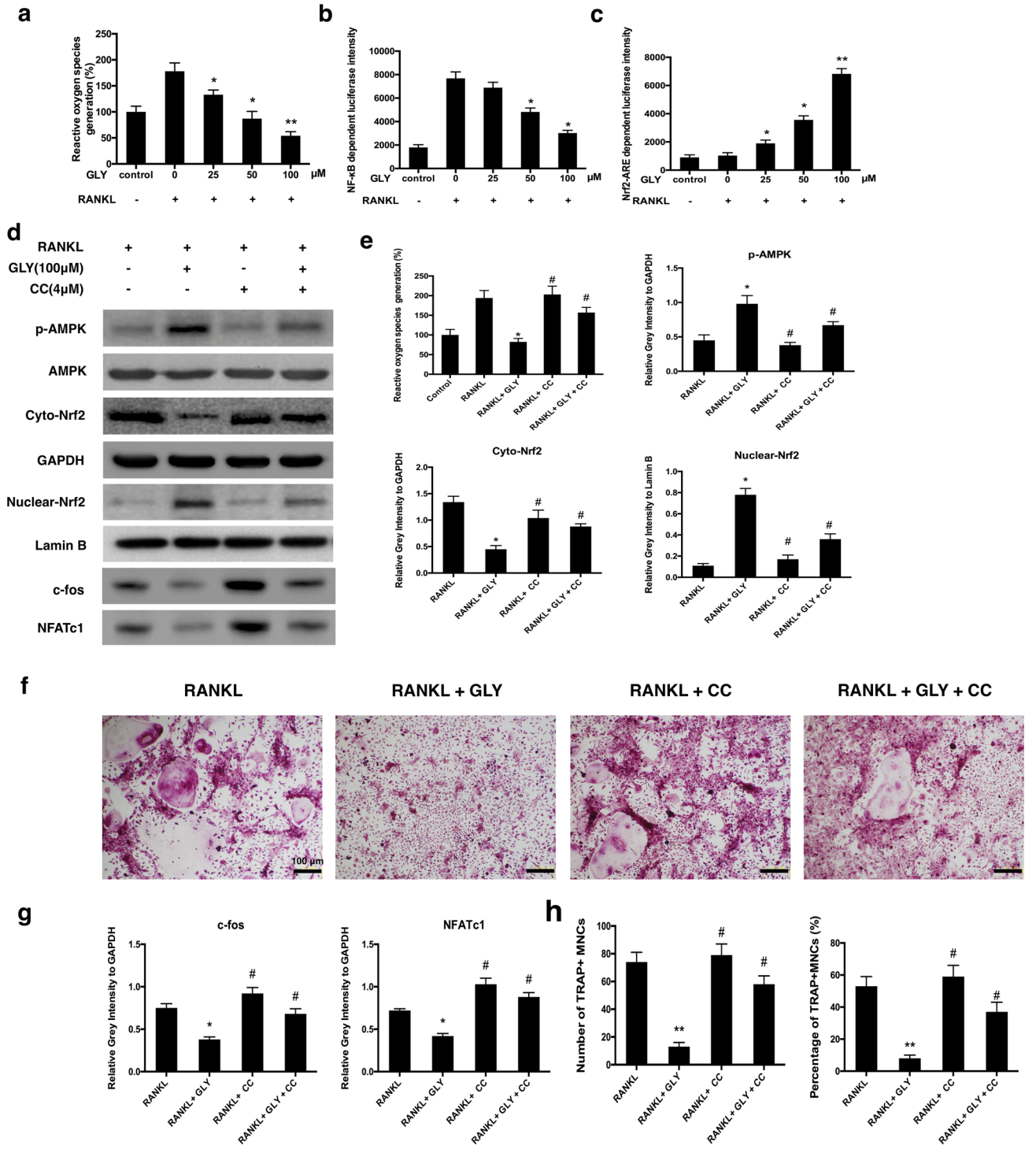

Fig. 5 Involvement of AMPK in Nrf2 nuclear distribution and antioxidation by glycyrrhizin. **a** ROS in pre-osteoclasts were detected using DCFH-DA with or without glycyrrhizin. **b, c** Luciferase activities of NF-kB and Nrf2-ARE were detected in RAW264.7 cells under the stimulation of RANKL and different concentrations of glycyrrhizin. **d, e** Activation of AMPK and Nrf2 in osteoclasts induced by RANKL were detected with or without glycyrrhizin or/and compound c (inhibitor of AMPK). **f, h** Formation of osteoclasts was evaluated by TRAP staining with or without glycyrrhizin or/and compound c. **g** Osteoclastogenesis-associated genes, c-fos and NFATc1, were detected as well. Asterisk indicates $p < 0.05$ when compared with RANKL group, double asterisk indicates $p < 0.01$, hash indicates $p < 0.05$ when compared with RANKL + GLY group

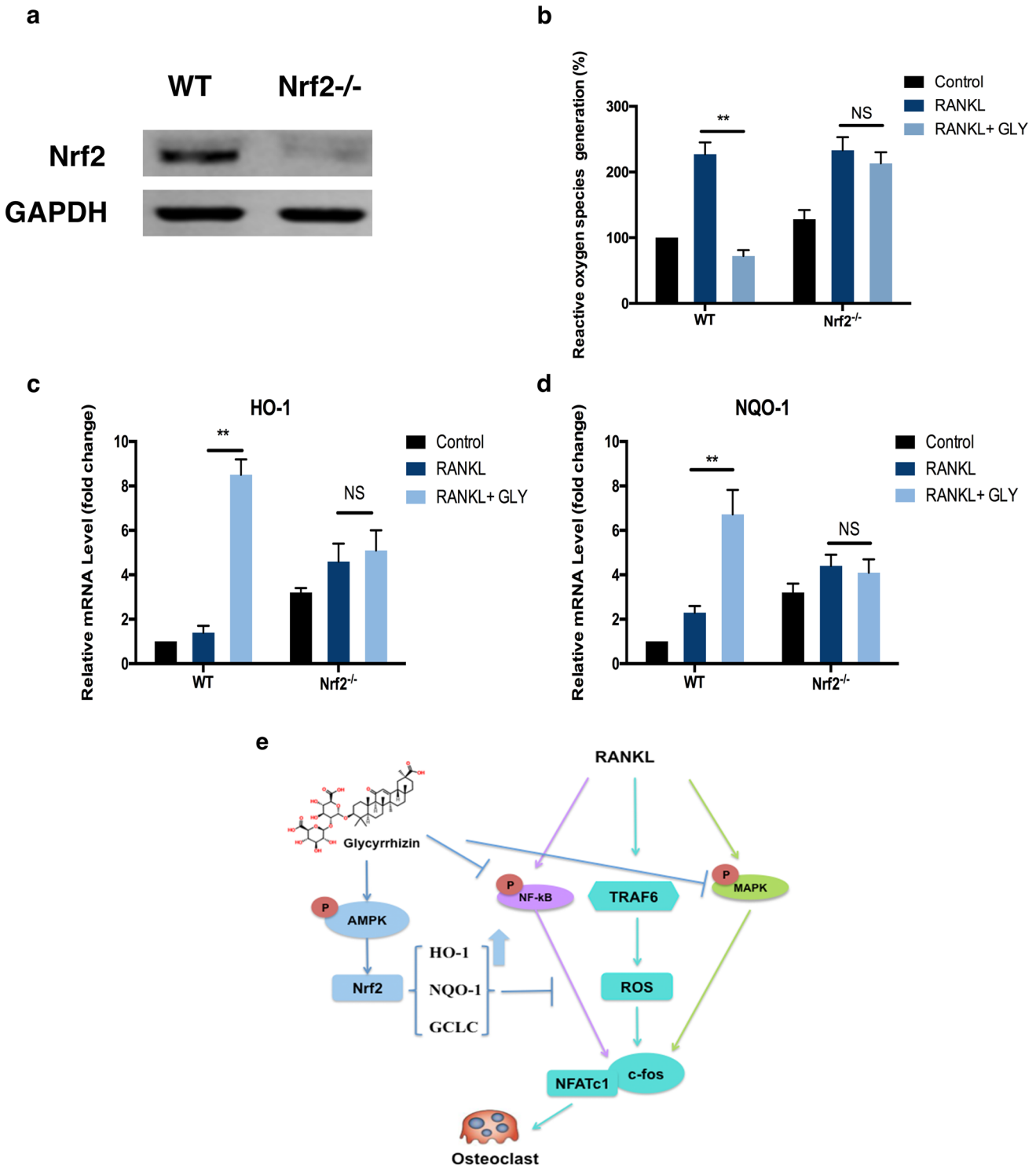

Fig. 6 Knockout of Nrf2 abolished the suppression of glycyrrhizin on oxidative stress caused by RANKL. **a** Proteins of Nrf2 were detected in wild-type (WT) and Nrf2$^{-/-}$ RAW 264.7 cells. **b** ROS were detected in both WT and Nrf2$^{-/-}$ with or without glycyrrhizin. **c, d** mRNA of HO-1 and NQO1 of WT and Nrf2$^{-/-}$ were investigated by RT-PCR in the presence and the absence of glycyrrhizin. Double asterisk indicates $p < 0.01$, *NS* indicates no significant differences. **e** Graphic abstract of molecular mechanisms of glycyrrhizin suppressing osteoclastogenesis and oxidative stress induced by RANKL. Phosphorylation of NF-κB, JNK, and p38 induced by RANKL were inhibited by glycyrrhizin while AMPK was activated and Nrf2/HO-1 was upregulated

shown to participate in the regulation of cellular energetic metabolism, oxidative stress, and Nrf2-HO-1 pathway [10, 11, 40]. We investigated the effect of glycyrrhizin on intracellular oxidative stress during its inhibition on osteoclastogenesis, and it turned out that glycyrrhizin significantly reduced ROS in osteoclasts. Moreover, GLY activated the phosphorylation of AMPK and upregulated nuclear Nrf2 and antioxidative genes, including HO-1, NQO-1, and GCLC, in a dose-dependent manner by glycyrrhizin. Compound C (Dorsomorphin), used as an AMPK inhibitor, attenuated the inhibitory effect of glycyrrhizin on osteoclastogenesis and oxidative stress, which further confirmed the activation of AMPK by GLY. Thereafter, siRNA targeted against Nrf2 was used to establish transient Nrf2 knockout RAW 264.7 cells ($Nrf2^{-/-}$). The ROS assay revealed that the inhibition of oxidative stress by GLY was rescued in $Nrf2^{-/-}$ cells. As expected, RT-PCR demonstrated that the promoted expression of HO-1 and NQO-1 by GLY was abolished when Nrf2 was knocked out. Conclusively, GLY reduced oxidative stress in RANKL-induced osteoclasts, thereby inhibiting osteoclastogenesis by activating the AMPK/Nrf2 axis.

GLY is known to inhibit the enzyme 11-ß-hydroxysteroid dehydrogenase type 2 in the adrenal gland. This causes a resultant cortisol-induced mineralocorticoid effect leading to elevations of serum sodium and reduction of serum potassium levels, which can lead to hypertension [41]. However, it is well known that every drug has both therapeutic and toxic effects depending on dosage and usage. For instance, arsenic trioxide (As_2O_3) is a very old toxin but as well as an effective antitumor drug. In addition, this present research was a really preliminary basic ex vivo investigation and it only can tell us that GLY indeed has an inhibitory effect on osteoclastogenesis, which means that side effects of GLY used for preventing bone resorption in vivo will be our next focus. Moreover, even though severe systematic side effects exist, GLY could be used locally in further research, like articular irrigation or intra-articular injection for OA or RA patients, to find out if it would decrease the influence of GLY on liver and adrenal gland. At least, given the cortisol-induced mineralocorticoid effect of GLY, it would be the optimal drug for therapy of patients suffering from both hypoaldosteronism and osteoporosis. Therefore, our study only came up with a pharmacologic effect of GLY on bone resorption and there are still many further works to be done before GLY could be used clinically in terms of appropriate usage and dosage.

In summary, as illustrated (Fig. 6e), our findings firstly and clearly showed that glycyrrhizin suppresses RANKL-induced osteoclastogenesis and oxidative stress through activating AMPK/Nrf2 and inhibiting NF-κB and MAPK. Therefore, glycyrrhizin may be a potential drug for the treatment of osteoporosis and other osteoclasts-related diseases.

Acknowledgements We thank the staff at Department of Orthopedic, Tongren Hospital, Shanghai Jiao Tong University School of Medicine.

Compliance with Ethical Standards

Conflict of interest Zhikun Li, Chao Chen, Xiaodong Zhu, Yifan Li, Ronghua Yu, Wei Xu declare that they have no conflict of interest.

Human and Animal Rights and Informed Consent This study was ethically approved by the Institutional Animal Care and Use Committee of Shanghai Jiao Tong University School of Medicine and performed in accordance with the criteria defined by the rules of the committee.

References

1. Kular J, Tickner J, Chim SM, Xu J (2012) An overview of the regulation of bone remodelling at the cellular level. Clin Biochem 45(12):863–873
2. Boyle WJ, Simonet WS, Lacey DL (2003) Osteoclast differentiation and activation. Nature 423(6937):337–342
3. Reuter S, Gupta SC, Chaturvedi MM, Aggarwal BB (2010) Oxidative stress, inflammation, and cancer: how are they linked? Free Radic Biol Med 49(11):1603–1616
4. Baek KH, Oh KW, Lee WY, Lee SS, Kim MK, Kwon HS et al (2010) Association of oxidative stress with postmenopausal osteoporosis and the effects of hydrogen peroxide on osteoclast formation in human bone marrow cell cultures. Calcif Tissue Int 87(3):226–235
5. Kim JH, Kim K, Kim I, Seong S, Kim N (2015) NRROS negatively regulates osteoclast differentiation by inhibiting RANKL-mediated NF-N:B and reactive oxygen species pathways. Mol Cells 38(10):904–910
6. Lee NK, Choi YG, Baik JY, Han SY, Jeong DW, Bae YS et al (2005) A crucial role for reactive oxygen species in RANKL-induced osteoclast differentiation. Blood 106(3):852–859
7. Kanzaki H, Shinohara F, Kanako I, Yamaguchi Y, Fukaya S, Miyamoto Y et al (2016) Molecular regulatory mechanisms of osteoclastogenesis through cytoprotective enzymes. Redox Biol 8:186–191
8. Wakabayashi N, Slocum SL, Skoko JJ, Shin S, Kensler TW (2010) When NRF2 talks, who's listening? Antioxid Redox Signal 13(11):1649–1663
9. Hasan MK, Friedman TC, Sims C, Lee DL, Espinoza-Derout J, Ume A et al (2018) Alpha-7-nicotinic acetylcholine receptor agonist ameliorates nicotine plus high-fat diet-induced hepatic steatosis in male mice by inhibiting oxidative stress and stimulating AMPK signaling. Endocrinology 159:931–944
10. Kumar R, Deep G, Wempe MF, Surek J, Kumar A, Agarwal R et al (2018) Procyanidin B2 3,3″-di-*O*-gallate induces oxidative stress-mediated cell death in prostate cancer cells via inhibiting MAP kinase phosphatase activity and activating ERK1/2 and AMPK. Mol Carcinog 57(1):57–69
11. Zhou X, He L, Zuo S, Zhang Y, Wan D, Long C et al (2018) Serine prevented high-fat diet-induced oxidative stress by activating AMPK and epigenetically modulating the expression of glutathione synthesis-related genes. Biochim Biophys Acta 1864(2):488–498
12. Oloyede HOB, Ajiboye HO, Salawu MO, Ajiboye TO (2017) Influence of oxidative stress on the antibacterial activity of betulin, betulinic acid and ursolic acid. Microb Pathog 111:338–344

13. Sadeghi A, Seyyed Ebrahimi SS, Golestani A, Meshkani R (2017) Resveratrol ameliorates palmitate-induced inflammation in skeletal muscle cells by attenuating oxidative stress and JNK/NF-kappaB pathway in a SIRT1-independent mechanism. J Cell Biochem 118(9):2654–2663
14. Tian Y, Ma J, Wang W, Zhang L, Xu J, Wang K et al (2016) Resveratrol supplement inhibited the NF-kappaB inflammation pathway through activating AMPKalpha-SIRT1 pathway in mice with fatty liver. Mol Cell Biochem 422(1–2):75–84
15. Zhao W, Li A, Feng X, Hou T, Liu K, Liu B et al (2016) Metformin and resveratrol ameliorate muscle insulin resistance through preventing lipolysis and inflammation in hypoxic adipose tissue. Cell Signal 28(9):1401–1411
16. Pellegrini GG, Morales CC, Wallace TC, Plotkin LI, Bellido T (2016) Avenanthramides prevent osteoblast and osteocyte apoptosis and induce osteoclast apoptosis in vitro in an Nrf2-independent manner. Nutrients. https://doi.org/10.3390/nu8070423
17. Thummuri D, Naidu VGM, Chaudhari P (2017) Carnosic acid attenuates RANKL-induced oxidative stress and osteoclastogenesis via induction of Nrf2 and suppression of NF-kappaB and MAPK signalling. J Mol Med (Berl) 95(10):1065–1076
18. Abo El-Magd NF, El-Mesery M, El-Karef A, El-Shishtawy MM (2018) Glycyrrhizin ameliorates high fat diet-induced obesity in rats by activating NrF2 pathway. Life Sci 193:159–170
19. Ekanayaka SA, McClellan SA, Barrett RP, Hazlett LD (2017) Topical glycyrrhizin is therapeutic for pseudomonas aeruginosa keratitis. J Ocul Pharmacol Ther. https://doi.org/10.1089/jop.2017.0094
20. Thakur V, Nargis S, Gonzalez M, Pradhan S, Terreros D, Chattopadhyay M (2017) Role of glycyrrhizin in the reduction of inflammation in diabetic kidney disease. Nephron 137(2):137–147
21. Zhang X, Yang H, Yue S, He G, Qu S, Zhang Z et al (2017) The mTOR inhibition in concurrence with ERK1/2 activation is involved in excessive autophagy induced by glycyrrhizin in hepatocellular carcinoma. Cancer Med 6(8):1941–1951
22. Wang C, Xiao F, Qu X, Zhai Z, Hu G, Chen X et al (2017) Sitagliptin, an anti-diabetic drug, suppresses estrogen deficiency-induced osteoporosisin vivo and inhibits RANKL-induced osteoclast formation and bone resorption in vitro. Front Pharmacol 8:407
23. Wu X, Li Z, Yang Z, Zheng C, Jing J, Chen Y et al (2012) Caffeic acid 3,4-dihydroxy-phenethyl ester suppresses receptor activator of NF-kappaB ligand-induced osteoclastogenesis and prevents ovariectomy-induced bone loss through inhibition of mitogen-activated protein kinase/activator protein 1 and Ca^{2+}-nuclear factor of activated T cells cytoplasmic 1 signaling pathways. J Bone Miner Res 27(6):1298–1308
24. Zeng XZ, He LG, Wang S, Wang K, Zhang YY, Tao L et al (2016) Aconine inhibits RANKL-induced osteoclast differentiation in RAW264.7 cells by suppressing NF-kappaB and NFATc1 activation and DC-STAMP expression. Acta Pharmacol Sin 37(2):255–263
25. Jin J, Xiong T, Hou X, Sun X, Liao J, Huang Z et al (2014) Role of Nrf2 activation and NF-kappaB inhibition in valproic acid induced hepatotoxicity and in diammonium glycyrrhizinate induced protection in mice. Food Chem Toxicol 73:95–104
26. Ito K, Jazrawi E, Cosio B, Barnes PJ, Adcock IM (2001) p65-activated histone acetyltransferase activity is repressed by glucocorticoids: mifepristone fails to recruit HDAC2 to the p65-HAT complex. J Biol Chem 276(32):30208–30215
27. Akanda MR, Park BY (2017) Involvement of MAPK/NF-kappaB signal transduction pathways: *Camellia japonica* mitigates inflammation and gastric ulcer. Biomed Pharmacother 95:1139–1146
28. Chan LP, Liu C, Chiang FY, Wang LF, Lee KW, Chen WT et al (2017) IL-8 promotes inflammatory mediators and stimulates activation of p38 MAPK/ERK-NF-kappaB pathway and reduction of JNK in HNSCC. Oncotarget 8(34):56375–56388
29. Choi JH, Han Y, Kim YA, Jin SW, Lee GH, Jeong HM et al (2017) Platycodin D inhibits osteoclastogenesis by repressing the NFATc1 and MAPK signaling pathway. J Cell Biochem 118(4):860–868
30. Wilson C. Bone (2014) Oxidative stress and osteoporosis. Nat Rev Endocrinol 10(1):3
31. Yang YH, Li B, Zheng XF, Chen JW, Chen K, Jiang SD et al (2014) Oxidative damage to osteoblasts can be alleviated by early autophagy through the endoplasmic reticulum stress pathway-implications for the treatment of osteoporosis. Free Radic Biol Med 77:10–20
32. Dharmapatni A, Algate K, Coleman R, Lorimer M, Cantley MD, Smith MD et al (2017) Osteoclast-associated receptor (OSCAR) distribution in the synovial tissues of patients with active RA and TNF-alpha and RANKL regulation of expression by osteoclasts in vitro. Inflammation 40:1566–1575
33. Chakraborty C, Doss CG (2013) Crucial protein based drug targets and potential inhibitors for osteoporosis: new hope and possibilities. Curr Drug Targets 14(14):1707–1713
34. Deal C (2009) Potential new drug targets for osteoporosis. Nat Clin Pract Rheumatol 5(1):20–27
35. Xu B, Lovre D, Mauvais-Jarvis F (2017) The effect of selective estrogen receptor modulators on type 2 diabetes onset in women: basic and clinical insights. J Diabetes Complic 31(4):773–779
36. Hsiao FY, Hsu WW (2017) Comparative risks for cancer associated with use of calcitonin, bisphosphonates or selective estrogen receptor modulators among osteoporosis patients: a population-based cohort study. Jpn J Clin Oncol 47(10):935–941
37. Zhou W, Lin L, Cheng Y, Liu Y (2017) Ursolic acid improves liver transplantation and inhibits apoptosis in miniature pigs using donation after cardiac death. Cell Physiol Biochem 43(1):331–338
38. Song MK, Park C, Lee YD, Kim H, Kim MK, Kwon JO et al (2018) Galpha12 regulates osteoclastogenesis by modulating NFATc1 expression. J Cell Mol Med 22:849–860
39. Wu M, Chen W, Lu Y, Zhu G, Hao L, Li YP (2017) Galpha13 negatively controls osteoclastogenesis through inhibition of the Akt-GSK3beta-NFATc1 signalling pathway. Nat Commun 8:13700
40. Zhao C, Zhang Y, Liu H, Li P, Zhang H, Cheng G (2017) Fortunellin protects against high fructose-induced diabetic heart injury in mice by suppressing inflammation and oxidative stress via AMPK/Nrf-2 pathway regulation. Biochem Biophys Res Commun 490(2):552–559
41. Omar HR, Komarova I, El-Ghonemi M, Fathy A, Rashad R, Abdelmalak HD et al (2012) Licorice abuse: time to send a warning message. Ther Adv Endocrinol Metab 3(4):125–138